



Luminescent properties of LiF crystals for fluorescent imaging of nuclear particles tracks

P. Bilski^{a,*}, B. Marczevska^a, W. Gieszczyk^a, M. Kłosowski^a, M. Naruszewicz^a,
Y. Zhydachevskyy^{b,c}, S. Kodaira^d

^a Institute of Nuclear Physics, Polish Academy of Sciences (IFJ PAN), 31-342, Kraków, Poland

^b Institute of Physics, Polish Academy of Sciences, PL-02668, Warsaw, Poland

^c Lviv Polytechnic National University, Lviv, 79646, Ukraine

^d National Institute of Radiological Sciences (NIRS), QST, Chiba, Japan

ARTICLE INFO

Keywords:

LiF
Photoluminescence
Fluorescent nuclear track detectors
Radiation measurements

ABSTRACT

Fluorescent nuclear track detectors (FNTD) based on LiF crystals were used for imaging ionizing particle tracks (including high-energy iron ions), by exploiting photoluminescence of radiation induced F_2 and F_3^+ color centers. The relation between photoluminescence emission spectrum of LiF and quality of FNTD images was investigated. It was found that in the applied experimental conditions, the emission within the green band (530 nm, F_3^+) is very weak compared to the red band (670 nm, F_2). The optimum signal to noise ratio was achieved with setting the measuring window at wavelengths longer than 570 nm. Good quality track images in the green spectral range were obtained only for the highest ionization density: for stopping iron ions.

Investigations of the bleaching phenomenon revealed a strong decrease of the PL intensity after long excitation times, in the range of several minutes. The amount of this decrease depends on the used excitation power. In the conditions which were typically applied during FNTD measurements the intensity loss was negligible.

1. Introduction

Lithium fluoride (LiF) is a well-known luminescent and optical material. The refractive index of LiF $n = 1.39$ is one of the lowest among dielectric materials, while energy band gap ~ 14 eV, one of the largest. LiF possesses one of the highest UV transmission among all materials. The luminescence effects in LiF have been studied and applied in practice for several decades. A lot of research was devoted to thermoluminescence (TL) of LiF. This compound was the first material used in practice for ionizing radiation thermoluminescent dosimetry [1]. Since that time several versions of LiF-based TL detectors were developed, differing in methods of synthesis, doping and properties. Two of them: LiF:Mg,Ti and LiF:Mg,Cu,P are probably the most widely used TL detectors in the world [2].

Another group of very interesting phenomena, which have been also studied for decades [3], is related to color centers in LiF and their photoluminescence (PL). Ionizing radiation creates in LiF F centers (anion vacancies trapping electrons), which tend to aggregate forming more complex defects. Among them of special interest are F_2 and F_3^+ color centers. F_2 center is composed of two anion vacancies with two

bounded electrons, while F_3^+ of three vacancies with two electrons. Both these centers have overlapped absorption bands peaked around 440–450 nm, while the photoluminescence emission spectrum exhibits two bands at about 670 nm (related to F_2) and about 530 nm (related to F_3^+). Photoluminescence of radiation induced color centers in LiF was applied for imaging [4–6], lasers [7–10] and high-dose dosimetry [11,12].

Recently, photoluminescence of F_2/F_3^+ centers in LiF was successfully exploited for microscopic imaging of tracks of single nuclear particles [13–15]. This technique was originally developed with $Al_2O_3:C,Mg$ crystals [16–18] and detectors based on it are called fluorescent nuclear track detectors (FNTD). FNTDs enable the visualization of nuclear particles tracks with the sub-micrometer resolution. Up to the mentioned recent works on LiF, $Al_2O_3:C,Mg$ remained the only successful FNTD.

In the present paper we discuss some luminescent and optical properties of LiF crystals and their impact on fluorescent imaging of nuclear tracks.

* Corresponding author.

E-mail address: pawel.bilski@ifj.edu.pl (P. Bilski).

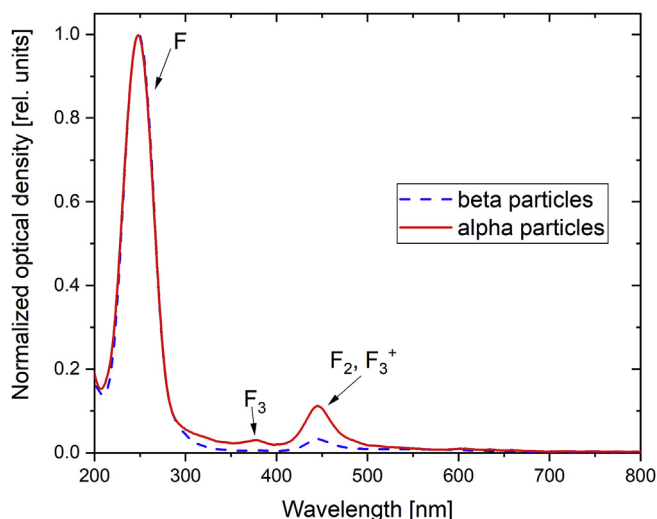


Fig. 1. LiF absorption spectra measured after irradiation of a crystal with alpha and beta particles, normalized to the maximum of F-center absorption band. Alpha particle fluence: $\sim 5.5 \times 10^{11} \text{ cm}^{-2}$ (c.a. 100 kGy). Beta-ray dose: 30 kGy.

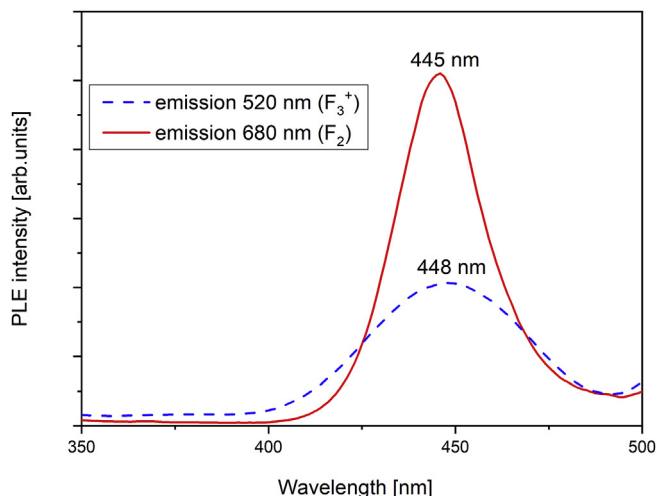


Fig. 2. Photoluminescence excitation spectra for F_2 and F_3^+ color centers in LiF crystal, measured after 1 kGy dose of beta radiation. (For interpretation of the references to color in this figure legend, the reader is referred to the Web version of this article.)

2. Materials and methods

LiF single crystals were grown at the IFJ PAN with the Czochralski method in argon atmosphere, using LiF powder, self-synthesized from HF and LiCl, as a starting material. The obtained transparent crystals were then cut with diamond saws into the desired size (typically square plates $4 \times 4 \times 1 \text{ mm}$) and polished with fine abrasive strips. Prior to further measurements, the crystal samples were pre-heated at temperature 820–830 °C for 10 min. This treatment improved quality of the crystal surface by removing small scratches left by polishing. The heating removed also possibly preexisting color centers.

Test irradiations were performed with isotopic sources: alpha particles (^{241}Am) and beta particles ($^{90}\text{Sr}/^{90}\text{Y}$). Irradiations with high-energy iron ions were carried out at the HIMAC accelerator in Chiba, Japan. The iron beam had the nominal energy of 500 MeV/nucleon, while the actual energy available in the experimental room was 412.5 MeV/nucleon. For some irradiations the beam energy was additionally decreased by using PMMA absorbers of various thickness. The energy at

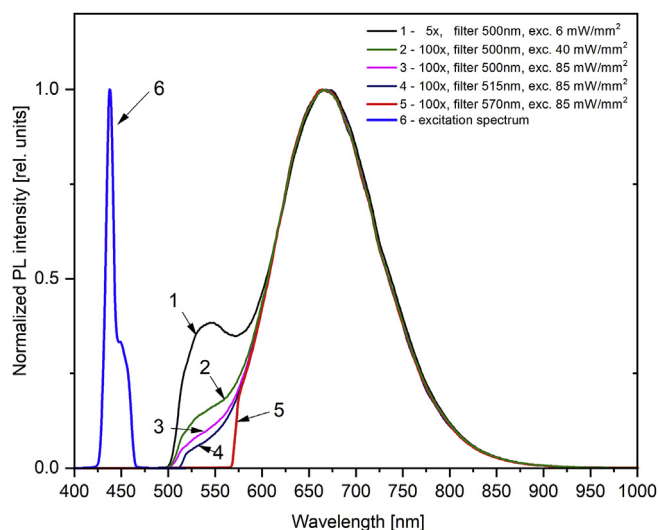


Fig. 3. Normalized PL emission spectra of the alpha irradiated LiF crystal, measured for various optical configuration (lenses, excitation intensity, filters). The applied spectrum of the excitation light is also presented.

the sample position, as well as LET values, were then calculated using SRIM code [19]. The particle fluence was 10^5 cm^{-2} .

Microscopic observations were conducted using a Nikon Eclipse Ni-U upright fluorescence wide-field microscope with a DS-Qi2 CCD camera. For excitation the Lumen 200 illumination system with metal halide lamp (Prior Scientific) was used. The illumination intensity at samples position was measured with the PM100 power and energy meter in conjunction with S170C Microscope Slide Photodiode Power Sensor (Thorlabs). A band-pass filter ET445/30 was used for excitation light, while various filters were applied for emission (see section 3). The most of observations were conducted with 100 × TU Plan ELWD (NA 0.80) objective lens, but 50 × TU Plan ELWD (NA 0.60) and 20 × PLAN APO (NA 0.75) were also applied. The Ni-U microscope may be used with two different settings of the distance between the lens and the CCD. At the short distance the amount of collected light is higher, but pixel size is larger ($0.07 \mu\text{m}$, instead of $0.03 \mu\text{m}$). Both options were used within this work, depending on the needs. Image analysis were realized with the Nikon NIS-Elements and with the Fiji software [20].

The photoluminescence excitation spectra were measured using a Horiba/Jobin-Yvon Fluorolog-3 spectrofluorometer with a 450 W xenon lamp and a Hamamatsu R928P photomultiplier. The photoluminescence emission spectra were measured using Ocean Optics QE pro 00689 spectrometer. In order to perform measurements in conditions possibly similar to those used for FNTD imaging, the spectrometer was mounted onto the microscope in place of the CCD camera and therefore using exactly the same light source, lenses, filters and dichroic mirrors. The optical absorbance spectra were measured using a Varian Cary 5000 UV-Vis-NIR spectrophotometer. All measurements were performed at room temperature and results were corrected for spectral response of the instruments.

3. Results and discussion

3.1. Spectral measurements

Measurements of photoluminescence emission and excitation, as well as absorption spectra, were conducted with the same LiF crystal samples as those used for FNTD imaging. The only difference was in the radiation doses (particle fluence), which must be much higher than in case of FNTDs, in order to produce a measurable signal intensity.

Fig. 1 compares LiF absorption spectra measured after irradiation with alpha and beta particles. As expected, the most dominant is F-

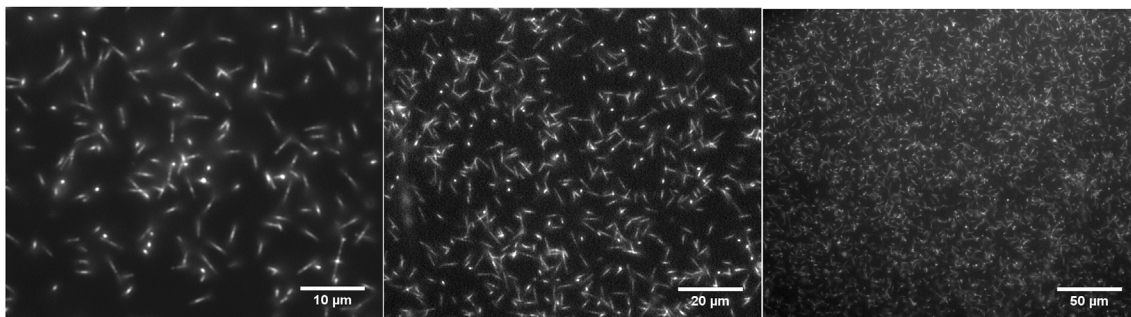


Fig. 4. Examples of images of alpha particles tracks (fluence $\sim 1.5 \times 10^6 \text{ cm}^{-2}$) for different objective lenses (from left): $100 \times / \text{NA}0.8$, $50 \times / \text{NA}0.6$, $20 \times / \text{NA}0.75$.

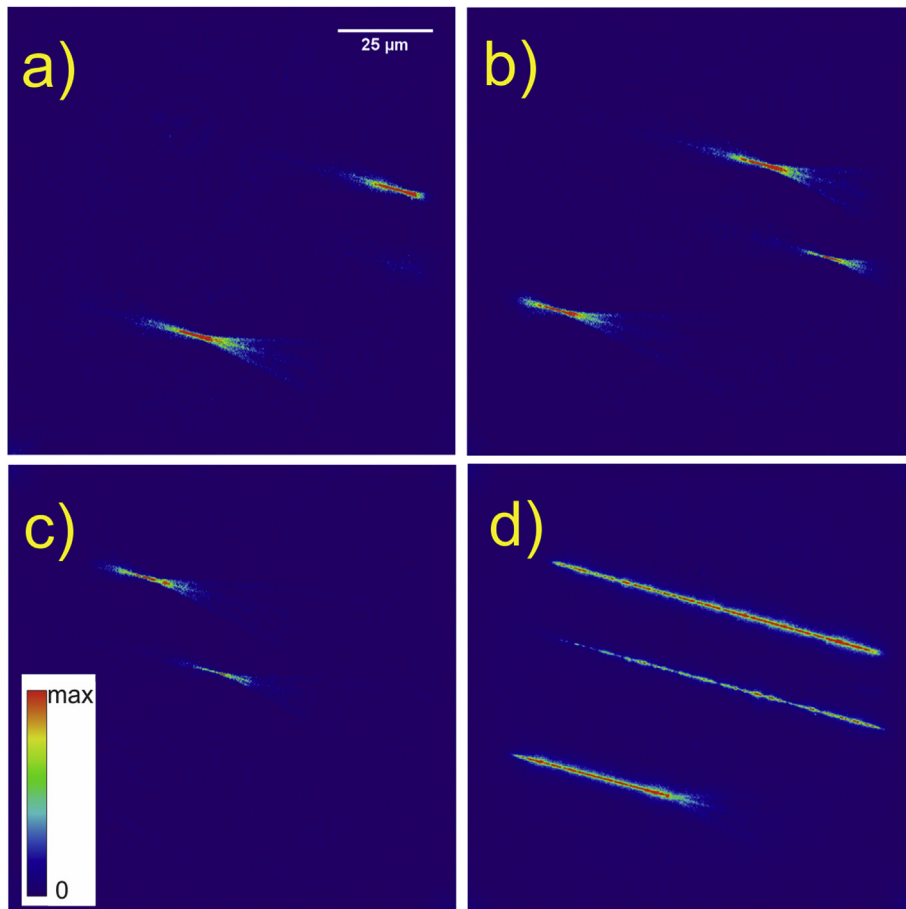


Fig. 5. Images of the iron ion tracks (energy 145 MeV/nucleon) registered at different depth into the crystal: a) depth 10 μm , b) depth 20 μm , c) depth 35 μm , d) maximum intensity projection of the whole stack of images (35 images from 10 μm to 45 μm with 1 μm step). Background of images was subtracted using Mosaic group plugin to Fiji software [25]. The color scale illustrates PL intensity (arbitrary units). (For interpretation of the references to color in this figure legend, the reader is referred to the Web version of this article.)

center band. The band at about 445 nm, corresponding to F_2 and F_3^+ centers, is well visible for both radiation modalities. It is interesting that this band is relatively higher after alpha particle irradiation than after beta-rays. This may be a result of the higher dose used for alpha particle irradiation (c.a. 100 kGy for alpha and 30 kGy for beta) or an effect of high ionization density within alpha particle tracks.

Fig. 2 presents the overlapped PL excitation spectra for F_2 and F_3^+ centers. The results agree well with the differences between both bands described in the literature: a small displacement between positions of band maxima and a wider shape of F_3^+ band [4].

While the general shape of LiF PL emission spectrum, consisting of bands located around 670 nm and 530 nm, is well known, the proportion between these two bands is not a constant value. Usually the red emission of F_2 is stronger, but one can find also published spectra with the dominant green F_3^+ band [21]. Their ratio depends not only on crystal properties and its irradiation history, but also on intensity and

wavelength of the excitation light. The influence of the excitation wavelength results directly from the differences in excitation spectra for F_2 and F_3^+ color centers (see Fig. 2). Less obvious is the effect of illumination intensity – a relative enhancement of F_2 band at high excitation intensities [22,23]. This phenomenon is explained by an increase of non-radiative transitions of F_3^+ centers at these conditions [24], which is observed as a kind of a saturation of PL vs. illumination intensity relationship for the band at 530 nm. Due to this variability of bands proportion, the emission spectra of LiF crystals were investigated with the optical set-up identical with that used for FNTD imaging.

The results of these measurements are illustrated in Fig. 3. The effect of illumination intensity on the emission spectrum is apparent (compare curves 1, 2 and 3). The curves 1 and 2 were measured with the same settings of the illumination system (10% of available power), but the effective irradiance was much higher in case of $100 \times$ lens, because the light was focused on a much smaller area. Consequently,

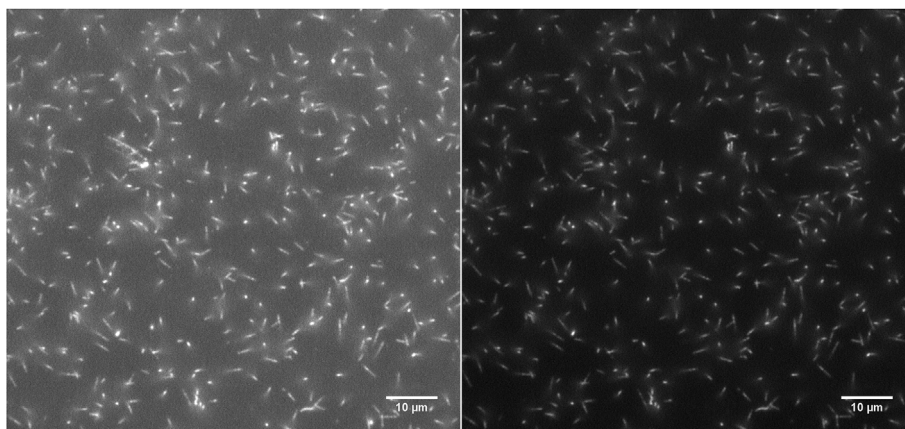


Fig. 6. Images of alpha particle tracks registered with different long-pass filters: 515 nm (left) and 570 nm (right) for the same LiF sample. Acquisition time 20 s, magnification 100 × .

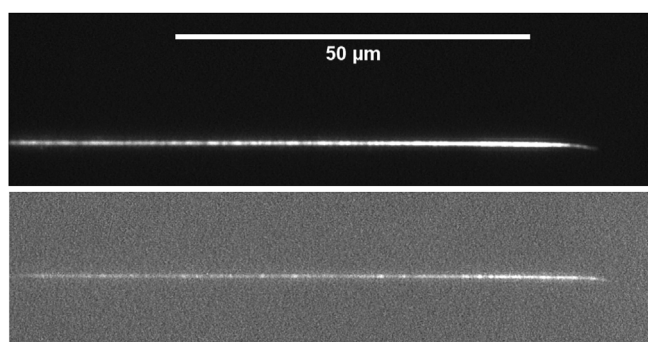


Fig. 7. Track of an iron ion stopping in the LiF crystal. Upper: filter LP570 (red), acquisition time 10s. Lower: filter 534/30 (green), acquisition time 40 s.

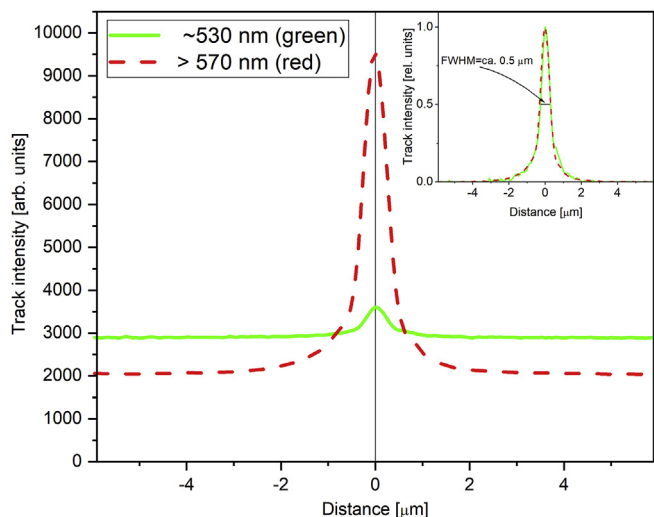


Fig. 8. Radial distribution of PL intensity across the track, measured for images from Fig. 7. In the inset: data after background subtraction and normalization to the maximum value (data processing with GlowView software [26]).

the 100 × lens produced less pronounced band at 530 nm than the 5 × lens. Fig. 3 compares also the performance of the several tested long-pass filters. The contribution of the F_3^+ band at the used optical set-up was found to be very low, therefore finally the 570 nm filter was mainly used for FNTD measurements, as it provides better separation from the excitation light than the 500 nm and 515 nm filters. This issue will be further discussed in section 3.2.

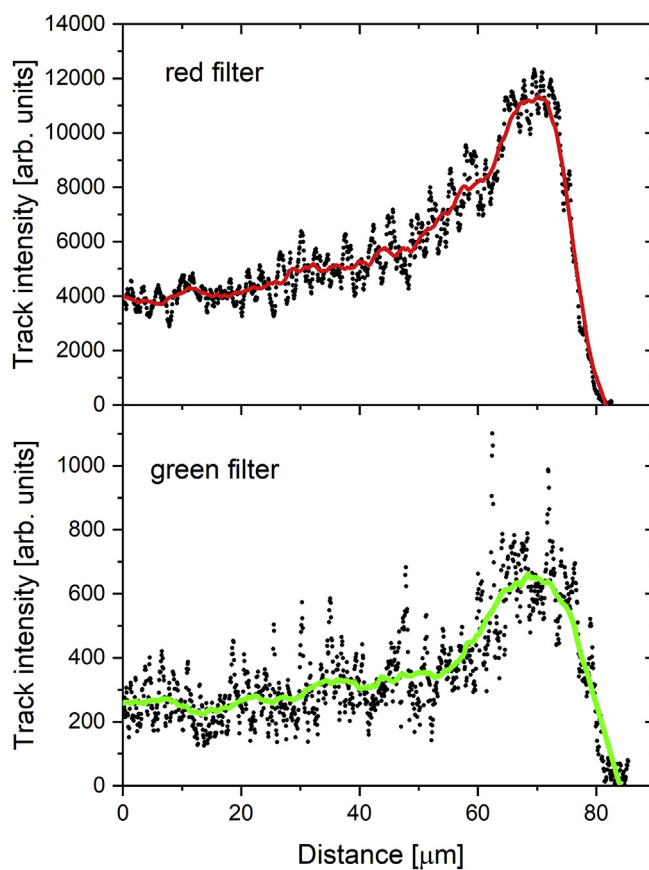


Fig. 9. Distribution of PL intensity along the track, measured for images from Fig. 7 (upper: filter LP570, lower: filter 534/30). Solid lines represent the smoothed data and are drawn only to guide the eye.

3.2. Fluorescent images of particle tracks

The main potential application of FNTDs is detection of densely ionizing particles (i.e. particles characterized by high linear energy transfer, LET). The radiation most convenient for testing purposes are alpha particles from isotopic sources, usually ^{241}Am . They have nominal energy exceeding 5 MeV, but due to energy loss in the source material, the actual energy spectrum of the applied source was broad, with the maximum at 3.5 MeV [15]. The range of such particles in LiF is only about 11 μm, while the LET in LiF varies from 290 keV/μm on entering crystal to 406 keV/μm in the Bragg peak. Fig. 4 presents

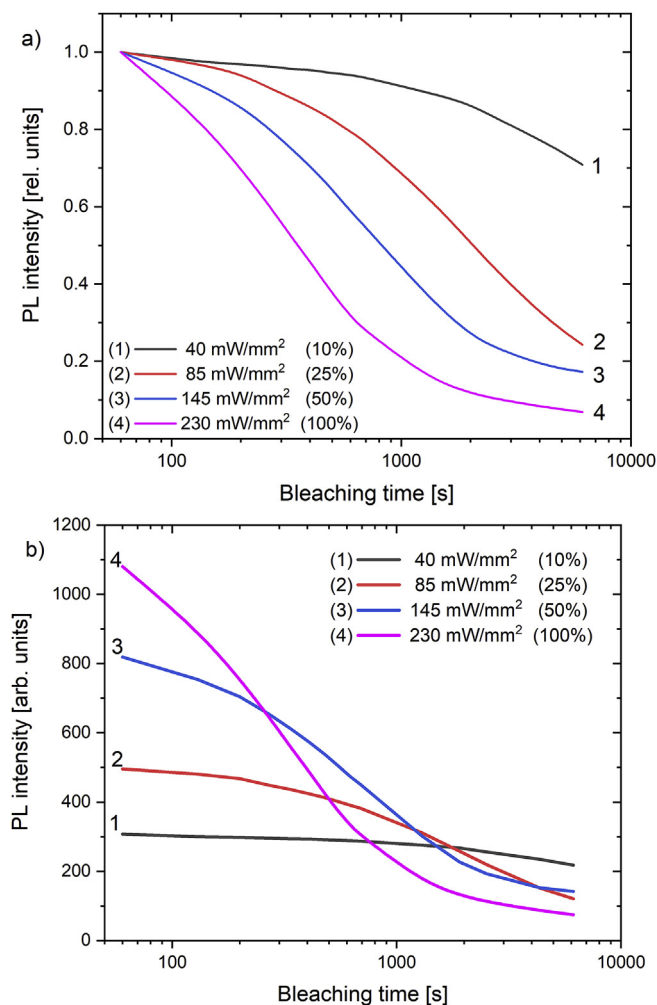


Fig. 10. Dependence of PL signal on the time of illumination, as measured for different relative illumination intensity. Objective lens $100\times$ /NA0.80, filter LP570. a) relative scale, b) absolute scale. The percentage values in parentheses indicate the nominal settings of the Lumen 200 illumination system.

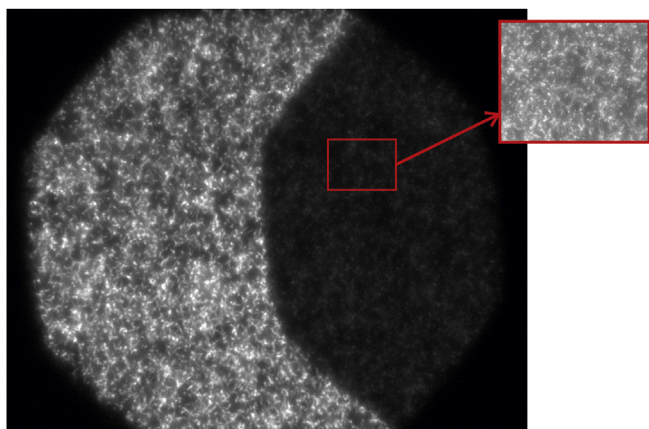


Fig. 11. Illustration of the effect of bleaching for about 6000 s illumination with intensity of 230 mW/mm^2 . The observed polygonal shape is due to the applied diaphragm in the path of the illumination light. The image was registered after executing the described photobleaching experiment and after shifting the LiF sample by approximately half of the field of view. The darker area represents the bleached region, while the bright area was not bleached. The inset shows an enlarged and brightened fragment of the bleached region.

examples of fluorescent images of alpha particles, which were acquired with different objective lenses. The best resolution is obviously achieved with the lens with the highest magnification and numerical aperture, and this objective was mainly used for the FNTD observation. However single alpha particle tracks can be also recognized even with the $20\times$ lens. Low magnification objectives might be useful in applications which require only counting of tracks, without analysis of their shape. An example of such application is neutron dosimetry, based on counting of very characteristic tracks created by products of nuclear reaction of neutrons with ^6Li nuclei [14]. It should be also mentioned that an improvement in resolution and image brightness may be still achieved by using immersion oil objectives, which can have numerical aperture up to 1.45.

The FNTDs are the best suited for detection of high-energy heavy ions. Recently an experimental campaign at the HIMAC accelerator in Chiba (Japan) was started, aimed on investigating of the performance of LiF FNTDs for the broad range of ion species and energies. In this work the first results of these investigations are presented, obtained for iron ion beams. Fig. 5 shows examples of images of tracks produced by iron ions with energy 145 MeV/nucleon. The ion beam was directed horizontally, almost in parallel to the crystal surface. This figure illustrates also the special feature of the used $100\times$ objective – a very short focal depth: below $1\ \mu\text{m}$. The effect of the short focal depth may be noticed already in Fig. 4a, where one can see that parts of track images are blurred. This out-of-focus light somewhat deteriorates the quality of an image. On the other hand, the short focal depth has also a very positive impact, as it allows for vertical sectioning of the crystal. Fig. 5a–c, present images acquired with focus set at different depth into the crystal. In that way, on each image another part of a track is visible and a stack of images is obtained. Such a stack may be then used for generating the maximum intensity projection picture, which shows the whole length of the track (Fig. 5d) or for reconstruction of 3D images.

As was shown in the section 3.1, the PL emission spectrum of LiF consists of two bands and extends from 500 nm to nearly 900 nm. While the green band was found in the applied experimental conditions to be much weaker than the red one, it was still necessary to verify the choice of the spectral window by direct measurements of fluorescent tracks. Fig. 6 presents images of alpha particle tracks registered with different long-pass filters: 515 nm and 570 nm, therefore including or not the green F_3^+ band. The image acquired comprising the green band is obviously brighter, but with less contrast due to higher background level. The ratio of fluorescence signal in the track and in the nearby unirradiated areas was found to be up to about 1.9 for 515 nm filter and 2.7 for 570 nm filter. For that reason the 570 nm filter was mainly applied in further measurements.

The earlier investigations of LiF PL spectra after alpha particle irradiation in comparison to those after beta exposure, indicated that F_3^+ green emission is relatively more intense for densely ionizing radiation [22]. While these investigations were carried out for high doses and their results not necessary translate to the level of single particle irradiation, it was worth trying to reveal some ionization density effects within tracks, by performing measurements in different spectral ranges. For this purpose a band-pass filter 534/30 nm was used. Unfortunately a small amount of luminescence light which is transmitted by this narrow filter, allowed for obtaining good quality images only for particles characterized by very high LET. The good example is the iron ion beam of energy about 66 MeV/nucleon, when entering LiF crystals. The range of ions with that energy in LiF is about 1.6 mm and the LET in LiF changes from $1394\text{ keV}/\mu\text{m}$ at the entrance into a sample, to $8963\text{ keV}/\mu\text{m}$ in the Bragg peak. The ion beam was directed horizontally to the surface of LiF plates of 4 mm in size, therefore the particles were stopping in the crystals. Fig. 7 presents images of the last $80\ \mu\text{m}$ of a track created by such stopping iron ion, measured within two spectral ranges: green and red. The track registered with the green filter seems to be thinner, but this is a misleading impression. The analysis of the transversal profile of the tracks (radial distribution of PL intensity)

revealed that both have the same shape and width of about $0.5\ \mu\text{m}$ (see inset in Fig. 8). Fig. 8 illustrates also the general problem with observations conducted within the green range: low intensity of the signal combined with a very high background.

Fig. 9 presents distribution of PL intensity along the track. In spite of the high fluctuations of the data points, the characteristic shape of a Bragg peak is distinctly visible in both cases. The ratio between maximum of the peak and values at the plateau is similar in both cases: 2.9 for the red range and 2.6 for the green. One may therefore conclude, that if any changes of the emission spectrum due to ionization density do exist, they seem to be too small to provide any advantage for FNTD analysis (at least with the presently available measurement set-up).

3.3. Bleaching

A photoluminescence measurement is basically a non-destructive process (oppositely to optically stimulated luminescence or thermoluminescence) and can be repeated on the same sample many times. However, a decrease of PL over a prolonged excitation is sometimes observed. In case of LiF, such effect – called bleaching, has been described in frame of investigations of LiF-based lasers [10,27]. The interpretation of bleaching is photoionization of F_2 centers, leading to creation of F_2^+ [28]. Several other photo-induced processes, as well as interactions between various centers and charge carriers are possible, including also recovery of F_2 centers by re-trapping released electrons [9,29]. The whole picture of processes occurring in an irradiated and illuminated LiF crystal is therefore complex and the magnitude of the bleaching effect depends on the concentrations of various defects in LiF crystal, as well as on wavelength and intensity of the excitation light. Occurrence of the bleaching may limit the possibility of using high light intensity or prolonged illumination times for acquiring fluorescent images. In order to clarify this issue, a series of bleaching experiments was performed using LiF crystals irradiated with a higher fluence of alpha particles ($\sim 10^8\ \text{cm}^{-2}$) and the microscope set-up used for FNTD measurements. The results, in terms of integrated luminescence output, are presented in Fig. 10. It is apparent that long illumination significantly decreases PL intensity. The scale of this decrease depends on the excitation intensity. It is however interesting that even the longest illumination time of nearly 2 h has not bleached completely the tracks, what is illustrated in Fig. 11. The longest acquisition time used for FNTD measurements is 120 s. Within this time, the $85\ \text{mW}/\text{mm}^2$ of light intensity produces a still negligible reduction of the PL signal. This value was therefore chosen as optimum, taking into account also the dependence of the signal intensity on excitation intensity, as it is illustrated in Fig. 10b.

4. Concluding remarks

LiF-based fluorescent nuclear track detectors are capable of imaging tracks produced by various ionizing particles. In this work the tracks created by high-energy iron ions were for the first time obtained. The measurements of the PL emission spectra performed using the microscope optics and illumination set-up, revealed that in this conditions the green emission band at 530 nm is very weak. The optimum signal to noise ratio is therefore achieved by setting the measuring window at wavelengths longer than 570 nm. A good quality track image in the green range was obtained only for the highest ionization density

(stopping iron ions).

Investigations of the bleaching phenomenon revealed a strong decrease of the PL signal after long excitation times: even 90% after 100 min at full available illumination intensity ($230\ \text{mW}/\text{mm}^2$). The degree of this decrease depends on the used excitation intensity. In the conditions which were typically applied during FNTD measurements, i.e. $85\ \text{mW}/\text{mm}^2$ of light intensity and acquisition times up to 120 s, the PL signal loss was negligible.

The directions of the further work seem to be twofold: on one hand attempts to increase signal intensity through crystals modifications and/or improvements in equipment and measuring procedures, and on the other hand developing methods of track analysis in order to extract some information on radiation quality.

Acknowledgements

This work was supported by the National Science Centre, Poland (Contract No. UMO-2015/17/B/ST8/02180).

References

- [1] F. Daniels, C.A. Boyd, D.F. Saunders, *Science* 117 (1953) 343.
- [2] P. Bilski, *Radiat. Protect. Dosim.* 100 (2002) 199–203.
- [3] J. Nahum, D.A. Wiegand, *Phys. Rev.* 154 (1967) 817–830.
- [4] R.M. Montoreali, F. Bonfigli, M. Piccinini, E. Nichelatti, M.A. Vincenti, *J. Lumin.* 170 (2016) 761–769.
- [5] T. Pikuz, A. Faenov, Y. Fukuda, M. Kando, P. Bolton, A. Mitrofanov, A. Vinogradov, M. Nagasono, H. Ohashi, M. Yabashi, K. Tono, Y. Senba, T. Togashi, T. Ishikawa, *Optic Express* 20 (2012) 3424–3433.
- [6] L. Reale, F. Bonfigli, A. Lai, F. Flora, P. Albertano, M.L. di Giorgio, L. Mezi, R.M. Montoreali, A. Faenov, T. Pikuz, S. Almaviva, M. Francucci, P. Gaudio, S. Martellucci, M. Richetta, A. Poma, *J. Microsc.* 258 (2015) 127–139.
- [7] G. Baldacchini, *J. Lumin.* 100 (2002) 333–343.
- [8] G. Baldacchini, R.M. Montoreali, *Opt. Mater.* 16 (2001) 53–61.
- [9] V.V. Ter-Mikirtychev, T. Tsuboi, *Prog. Quant. Electron.* 20 (1996) 219–268.
- [10] R. Boyd, J. Owen, K. Teegarden, *IEEE J. Quantum Electron.* 14 (1978) 697–697.
- [11] W.L. McLaughlin, *Radiat. Protect. Dosim.* 66 (1996) 197–200.
- [12] S.D. Miller, M.K. Murphy, M.R. Tinker, A. Kovács, W. McLaughlin, *Radiat. Protect. Dosim.* 101 (2002) 53–58.
- [13] P. Bilski, B. Marczevska, W. Gieszczyk, M. Kłosowski, T. Nowak, M. Naruszewicz, *Radiat. Protect. Dosim.* 178 (2018) 337–340.
- [14] P. Bilski, B. Marczevska, M. Kłosowski, W. Gieszczyk, M. Naruszewicz, *Radiat. Meas.* 116 (2018) 35–39.
- [15] P. Bilski, B. Marczevska, *Nucl. Instr. and Meth. B* 392 (2017) 41–45.
- [16] G.M. Akselrod, M.S. Akselrod, E.R. Benton, N. Yasuda, *Nucl. Instr. and Meth. B* 247 (2006) 295–306.
- [17] M.S. Akselrod, G.J. Sykora, *Radiat. Meas.* 46 (2011) 1671–1679.
- [18] S. Greilich, J.M. Osinga, M. Niklas, F.M. Lauer, G. Klimpki, F. Bestvater, J.A. Bartz, M.S. Akselrod, O. Jakel, *Radiat. Meas.* 56 (2013) 267–272.
- [19] J.F. Ziegler, M.D. Ziegler, J.P. Biersack, *Nucl. Instr. and Meth. B* 268 (2010) 1818–1823.
- [20] J. Schindelin, I. Arganda-Carreras, E. Frise, V. Kaynig, M. Longair, T. Pietzsch, S. Preibisch, C. Rueden, S. Saalfeld, B. Schmid, J.-Y. Tinevez, D.J. White, V. Hartenstein, K. Eliceiri, P. Tomancak, A. Cardona, *Nat. Methods* 9 (2012) 676.
- [21] G. Baldacchini, E. De Nicola, G. Giubileo, F. Menchini, G. Messina, R.M. Montoreali, A. Scacco, *Nucl. Instrum. Methods B* 141 (1998) 542–546.
- [22] P. Bilski, B. Marczevska, Y. Zhydashchevskii, *Radiat. Meas.* 97 (2017) 14–19.
- [23] L. Oster, S. Druzhyna, Y.S. Horowitz, *Nucl. Instr. and Meth. A* 648 (2011) 261–265.
- [24] G. Baldacchini, M. Cremona, G. d'Auria, R.M. Montoreali, V. Kalinov, *Phys. Rev. B* 54 (1996) 17508–17514.
- [25] J. Cardinale, *Histogram-based Background Subtractor for ImageJ*, ETH Zurich, 2010.
- [26] W. Gieszczyk, P. Bilski, *Radiat. Meas.* 107 (2017) 102–110.
- [27] Z. Błaszczak, M. Ludwiczak, F. Kaczmarek, *Phys. Status Solidi* 75 (1983) K195–K198.
- [28] T. Tsuboi, V.V. Ter-Mikirtychev, *Optic Commun.* 116 (1995) 389–392.
- [29] V.V. Ter-Mikirtychev, *J. Phys. Chem. Solid.* 58 (1997) 365–373.